

## Interactions between Carrageenans and Milk Proteins: A Microstructural and Rheological Study

D. Arltoft,<sup>†,‡</sup> R. Ipsen,<sup>\*,‡</sup> F. Madsen,<sup>†</sup> and J. de Vries<sup>†</sup>

Danisco A/S, Edwin Rahrs vej 38, 8220 Brabrand, Denmark, and Department of Food Science, Faculty of Life Sciences, University of Copenhagen, Rolighedsvej 30, 1958 Frederiksberg, Denmark

Received November 20, 2006; Revised Manuscript Received December 14, 2006

Gels were produced using  $\kappa$ -,  $\iota$ -, or hybrid-carrageenan at a low (0.2–0.25%) and a high (0.7–1.0%) dosage in skim milk. The microstructure of carrageenan and protein was observed by confocal laser scanning microscopy using direct immunostaining. Additionally, rheology was used to characterize the gels. The low  $\kappa$ - and  $\iota$ -carrageenan dosages resulted in gels with a fine stranded carrageenan–protein microstructure and emulsion-like inclusions, while the high dosages resulted in strongly flocculated microstructures. Hybrid-carrageenan exhibited flocculation at both dosages. When using  $\iota$ - and hybrid-carrageenan at a high dosage and  $\kappa$ -carrageenan at both dosages, the gel characteristics were dominated by carrageenan–carrageenan interactions. On the other hand, the gel with a low dosage of  $\iota$ -carrageenan in milk was barely fusible, indicating the presence of a true coupled network. We suggest that  $\kappa$ -,  $\iota$ -, and hybrid-carrageenan all interact with casein micelles but that the impact of this interaction on the total gel properties varied.

### Introduction

Carrageenans are sulfated polysaccharides obtained from red seaweed and are classified according to three types— $\lambda$ -,  $\iota$ -, and  $\kappa$ -carrageenan—depending on the number of sulfate groups per repeating disaccharide unit of  $\beta$ -1,3- and  $\alpha$ -1,4-linked galactose residues (three, two, and one, respectively). Hybrid-carrageenans are mixed chains with  $\iota$ - and  $\kappa$ -carrageenan repeating units in each molecule.<sup>1</sup> The sulfate groups impose a negative charge on the carrageenan, affecting its functionality.<sup>2</sup>  $\lambda$ -Carrageenan does not gel, and  $\iota$ -carrageenan forms soft, elastic gels, while  $\kappa$ -carrageenan forms strong, brittle gels. Gel formation of  $\iota$ -carrageenan in aqueous solutions occurs by a coil-to-helix transformation. For  $\kappa$ -carrageenan, gel formation depends on a further association of the double helices.<sup>3,4</sup>

Carrageenans are used extensively to gel dairy products as they are able to stabilize and gel milk proteins at a low dosage—0.03% for  $\kappa$ -carrageenan<sup>5</sup> and 0.05% for  $\iota$ -carrageenan.<sup>6</sup> Investigations using scanning electron microscopy,<sup>7</sup> electron microscopy,<sup>8</sup> rheology,<sup>5</sup> electrophoretic mobility, and diffusion coefficients<sup>9</sup> have indicated that this effect is caused by a direct interaction between the casein micelle and the  $\kappa$ - or  $\iota$ -carrageenan. A similar low dosage of carrageenan is unable to gel permeate from milk that has undergone ultra-filtration (i.e., a solution of the exact same ionic composition but without casein micelles). This phenomenon, called milk reactivity,<sup>10</sup> has been explained by the direct interaction between the negatively charged carrageenan helices and the  $\kappa$ -casein situated on the periphery of the casein micelle.<sup>9,11,12</sup>

In milk, behavioral differences exist between  $\kappa$ -carrageenan and  $\iota$ -carrageenan: the gel setting temperature ( $T_{\text{gel}}$ ) is  $\sim 36$  °C for 0.2%  $\kappa$ -carrageenan<sup>13</sup> as compared to  $\sim 47$  °C for 0.1%  $\iota$ -carrageenan.<sup>6</sup> Differences in the melting profiles have also been reported: 0.2%  $\kappa$ -carrageenan–milk gel melted at 57 °C,<sup>13</sup> while

0.1%  $\iota$ -carrageenan–milk gel melted above 70 °C.<sup>6</sup> Furthermore, the presence of casein micelles does not seem to influence the gelation temperature of  $\kappa$ -carrageenan,<sup>13</sup> whereas the gelation temperature of  $\iota$ -carrageenan increases by 8 °C in the presence of micellar casein as compared to milk permeate.<sup>6,14</sup> Such differences suggest that the mode and impact of interaction with the casein micelle is not the same for the two types of carrageenan.

Although the microstructure and mechanisms of carrageenan–gel formation in milk systems has been thoroughly discussed in existing publications, the lack of specific probes has resulted in far more indirect<sup>5,6,9,11,14–16</sup> than direct studies<sup>7,8,17</sup> of the carrageenan microstructure. A few of the previous studies have used covalently labeled carrageenan, and of these, none investigated the texture of the carrageenan gels.<sup>18,19</sup> Furthermore, no images of a hybrid-carrageenan–gel microstructure appear to have been published.

Hence, the objective of this study was to investigate the microstructural and rheological behavior of  $\kappa$ -,  $\iota$ -, and hybrid-carrageenan at low and high dosages in skim milk. In doing so, the aim was to increase the knowledge of carrageenan's milk reactivity.

To characterize the microstructure of the carrageenans, direct immunostaining was applied.<sup>20</sup> The use of antibodies as markers for specific structures traditionally involves a primary antibody with affinity for the antigen of interest and a secondary antibody conjugated with a fluorophore with affinity for the primary antibody.<sup>21</sup> This technique requires washing of the sample after each antibody addition. The direct immunostaining method, however, only employs a primary antibody conjugated with a fluorophore. We are only aware of one study employing direct immunostaining without subsequent washing. Here, the technique was successfully used for in vivo detection of colorectal carcinoma with the aid of endoscopy.<sup>22</sup> The direct immunostaining technique requires no washing step, which makes it possible to evaluate fully hydrated samples and to avoid artefacts produced by fixation, drying, or slicing processes. However, the signal-to-noise ratio can be an issue, and the technique also

\* To whom correspondence should be addressed. E-mail: ri@life.ku.dk. Phone: +45 3528 3225.

<sup>†</sup> Danisco A/S.

<sup>‡</sup> Department of Food Science, Faculty of Life Sciences, University of Copenhagen.

**Table 1.** Gel Compositions

gel name	carrageenan type	dosage (%)
KM1	$\kappa$	0.2
KM2	$\kappa$	0.7
IM1	$\iota$	0.25
IM2	$\iota$	1.0
HM1	hybrid	0.25
HM2	hybrid	0.8

implies that the antibody must retain its functionality in the environment present in the specimen. The polyclonal anti-carrageenan antibody has previously been shown to retain its affinity for carrageenan when tested in environments relevant to dairy products.<sup>20</sup>

## Materials and Methods

The carrageenans used in this study were all fully alkali-modified. The  $\kappa$ -carrageenan was from *Kappaphycus alvarezii* and had a molecular weight (MW) of 550 kDa, as determined by high-pressure size exclusion chromatography (HPSEC). The  $\kappa$ -carrageenan contained about 5%  $\iota$ -carrageenan (according to capillary electrophoresis, CE). The  $\iota$ -carrageenan was from *Eucheuma denticulatum*, had a MW (HPSEC) of about 650 kDa, and contained about 5% hybrid-carrageenan (CE). The hybrid-carrageenan was from *Gigartina skottsbergii*, with a MW (HPSEC) of about 610 kDa containing ~75%  $\kappa$ - $\iota$ -hybrid-carrageenan (2  $\kappa$ /3  $\iota$ ) (CE), ~5%  $\kappa$ -carrageenan, ~5%  $\lambda$ -carrageenan, and ~15% unknown carrageenan types. The carrageenans were all kindly provided by Danisco A/S (Brabrand, Denmark).

Carrageenan gels were made using fresh skim milk with 0.1% fat (Arla Foods, Viby J., Denmark).

**Gel Preparation.** The gels were made by suspending carrageenan at room temperature in 450 mL of milk. The solution was heated to 85 °C, followed by the addition and mixing of 2 mL of 12.5% NaN<sub>3</sub> into the solution to avoid microorganism growth. Subsequently, the solutions were filled into 155 mL plastic beakers, cooled in a 4 °C water bath overnight, and stored at 4 °C until use. The low carrageenan dosages in the samples were selected to ensure a gel where the carrageenan–protein actions, if present, would dominate. The high carrageenan concentration was chosen to ensure a firm gel where carrageenan–carrageenan interactions would dominate (Table 1). Each gel was prepared in two true replicates (i.e., two separate solutions).

**Large Deformation Characteristics.** The gels' texture parameters were determined using a texture analyzer TA-XT2i (Stable Microsystems, Surrey, UK) mounted with a 1/2 inch cylindrical probe, which penetrated 20 mm into the product. A force–time curve was obtained at a crosshead speed of 0.5 mm/s. Firmness was determined as the maximum resistance to the probe (i.e., the height of the force peak at initial fracture). Penetration depth at fracture was also assessed as a measure of gel flexibility. Each true replicate was measured once.

**Small Deformation Characteristics.** Gel samples for small amplitude oscillatory shear analyses were prepared by inverting the beakers filled with gel into the aperture of a 2 mm high plastic mould. A metal wire was used to cut 2 mm high gel slices along the surface of the mold. The second slice from each gel was used for punching out the discs of gel with a diameter of 25 mm used for analysis. A Stresstech Rheometer (Reologica AB, Lund, Sweden) with a serrated plate–serrated plate geometry was utilized. Prior to the analyses, a 5 min equilibration time was included. All measurements were performed once for each true replicate.

Stress sweeps were made at 5 °C from 0.01 Pa until critical stress was reached. To examine the presence of different gel types further (carrageenan–carrageenan, carrageenan–protein), melting profiles were assessed from 5 to 85 °C at 1 °C/min at a constant strain of 0.005. Stress sweeps were initially performed at 5 and 60 °C to ensure that the stress during melting profiles was, at all times, within the viscoelastic region.

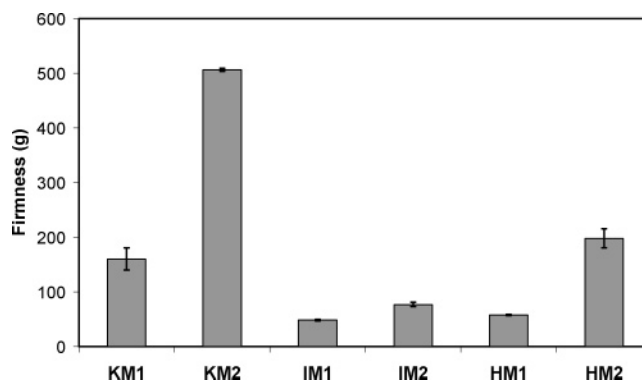


**Figure 1.** Large deformation firmness of gels measured with a texture analyzer. Abbreviations as in Table 1. Bars indicate standard deviation.

**Confocal Laser Scanning Microscopy (CLSM).** An inverted Leica TSP2 CLSM (Leica, Mannheim, Germany) with an argon/krypton and a helium/neon laser with a HCX PL APO 40× NA 1.2 oil immersion objective was used. Proteins were stained with 1  $\mu$ g of fluorescein isothiocyanate (FITC) dissolved in acetone (0.1 mg/mL). FITC was excited at 488 nm, and the emission was collected at 500–540 nm. The carrageenan was stained with ~10  $\mu$ g of anti-carrageenan antibody conjugated with Alexa Fluor 633 (~1 mol Alexa Fluor 633/mol of antibody) dissolved in 10 mM phosphate-buffered saline. The purification, conjugation, separation, and validation procedures have been described elsewhere.<sup>20</sup> The anti-carrageenan antibody was excited at 633 nm, and the emission was collected at 665–800 nm. FITC dissolved in acetone was applied to approximately 2 cm<sup>2</sup> of the cover glass. When the acetone had evaporated, the anti-carrageenan antibody was added to the same area, and a slice of gel was gently removed with a sharpened spatula (ca. 20 mm × 15 mm × 4 mm) and placed on the cover slip, covering the stains. FITC-conjugated polyclonal rabbit antibody F9387 (Sigma, Brøndby, Denmark) was used as a negative control antibody, as it binds to rat antibodies, which were not present in the gels. This made it possible to evaluate how antibodies were distributed in the sample when no specific binding was present and whether the structure indicated by the anti-carrageenan antibody was caused by specific binding. Following stain addition, the gels were left to incubate for at least 30 min at 15 °C. A temperature control stage was used at 15 °C. Ten images were recorded for each true replicate.

**Statistical Analysis.** Microsoft Excel software 2000 was employed to perform t-test for the comparison of large deformation gel strengths.

## Results

**Large Deformation Characteristics.** The gels spanned a wide range of textures, ranging from the bland and flexible gel with low  $\iota$ -carrageenan dosage to the very firm gel obtained with the high  $\kappa$ -carrageenan dosage (Figure 1). The increase in gel firmness was similar to the increase in carrageenan dosage for hybrid- and  $\kappa$ -carrageenan, whereas for  $\iota$ -carrageenan, the increase was much smaller. A 4-fold increase in  $\iota$ -carrageenan dosage resulted in a less than 2-fold increase in gel firmness.

The gels' penetration depth at fracture is shown in Figure 2. The  $\iota$ -carrageenan gels exhibited generally the highest penetration depth at fracture. For  $\kappa$ - and  $\iota$ -carrageenan, the increase in dosage did not alter the penetration depth at fracture significantly, whereas the high dosage of hybrid-carrageenan resulted in a significantly higher penetration depth at fracture ( $P < 0.01$ ) as compared to the low dosage.

**Small Amplitude Oscillatory Measurements. Stress Sweeps.** Figure 3 shows the stress sweeps of all gels. As expected, the  $\kappa$ -carrageenan gels had a higher complex modulus in the linear viscoelastic region ( $G^*_{lin}$ ) than  $\iota$ - and hybrid-carrageenan. With

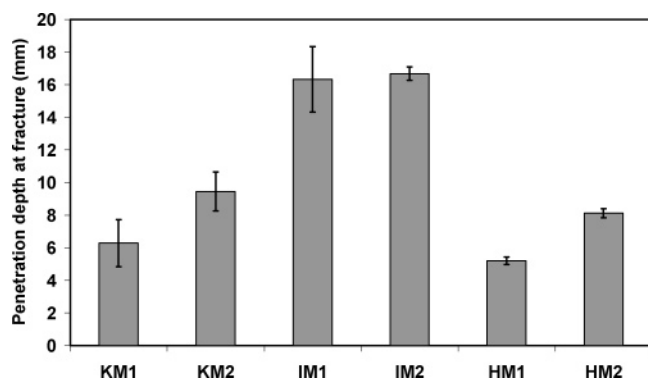


**Figure 2.** Penetration depth at fracture (mm) as determined by texture analyzer. Abbreviations as in Table 1. Bars indicate standard deviation.

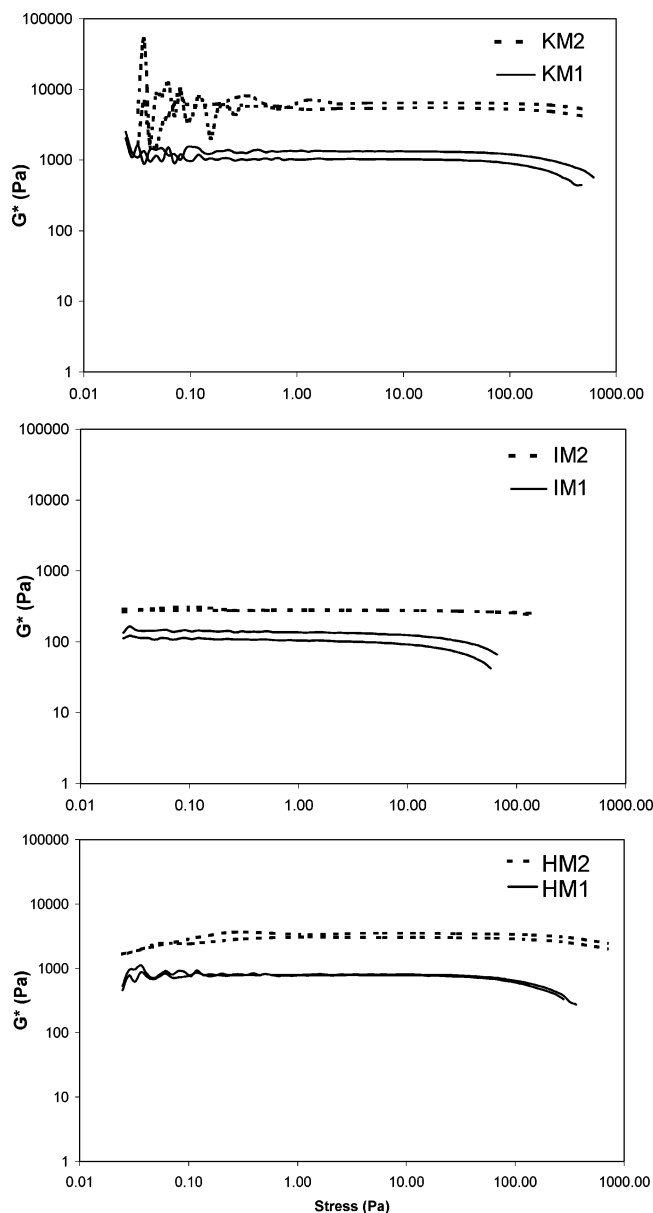


**Figure 3.** Stress sweeps of gels at 5 °C in replicate. Abbreviations as in Table 1.

the corresponding dosage,  $\iota$ -carrageenan exhibited a lower  $G^*_{lin}$  than both  $\kappa$ - and hybrid-carrageenan. The difference in  $G^*_{lin}$  between low and high dosages of  $\iota$ -carrageenan in milk was

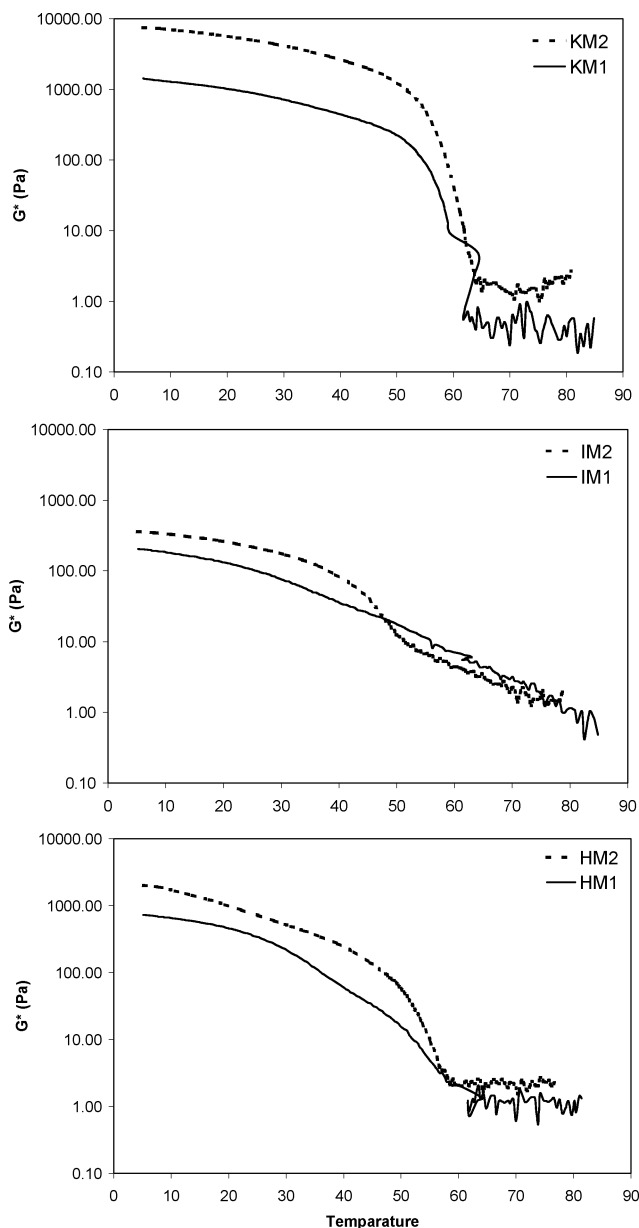


**Figure 4.** Melting profiles of  $\kappa$ -,  $\iota$ -, and hybrid-carrageenan gels from 5 to 85 °C at 1 °C/min. Each line represents the average of two replicates. The mean coefficient of variation was 10% between replicates.

only 2-fold, whereas, for  $\kappa$ - and hybrid-carrageenan, this difference corresponded to the increase in concentration. This is in agreement with the results from large deformation measurements and indicated that the gels formed at high and low  $\iota$ -carrageenan dosages must be of a different nature.

**Melting Profiles.** The melting profiles of the  $\kappa$ -carrageenan gels (Figure 4) showed a steep gradient, very different from the low dosage of  $\iota$ -carrageenan, which exhibited a melting profile with a very slow, steady decrease in  $G^*$  as a function of increasing temperature (Figure 4).

The gels made with hybrid-carrageenan exhibited a combination of  $\iota$ - and  $\kappa$ -characteristics. At a low dosage, the decrease in  $G^*$  was slow and gradual, as for the low dosage  $\iota$ -carrageenan, while the high dosage exhibited a steep decrease from ~50 °C. Above ~58 °C, the  $G^*$  of the hybrid-carrageenan gels did not decrease further, indicating a total breakdown of the gel



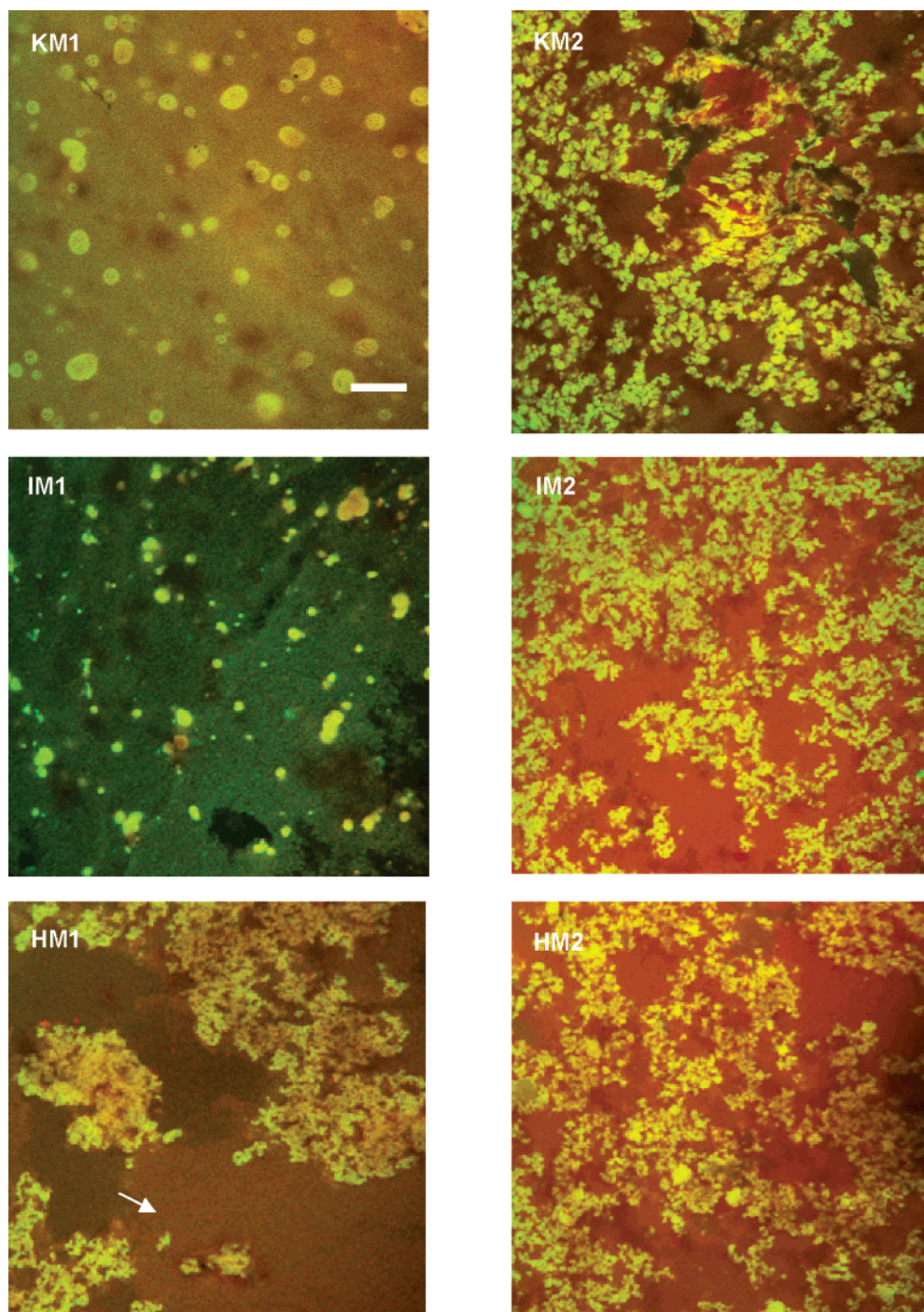


**Figure 5.** Representative low magnification CLSM images of the microstructure of carrageenan-milk gels. Abbreviations as in Table 1. Scale bar represents 50  $\mu\text{m}$ . Green is protein stained with FITC. Red is carrageenan stained with Alexa Fluor 633 conjugated anti-carrageenan antibody. All images have the same magnification as KM1. The arrow in HM1 shows the continuous phase, which resembles the structure of the continuous phase in KM1 and IM1.

structure, similar to the  $\kappa$ -carrageenan gels. No melting profiles of hybrid-carrageenan-milk gels appear to have been published previously.

**Microstructure.** A low dosage of  $\kappa$ - and  $\iota$ -carrageenan produced gels with a similar microstructure on the scale visualized by CLSM (Figures 5 and 6: KM1 and IM1). The continuous phase appeared to have a fine-stranded structure (1–3  $\mu\text{m}$  in length for  $\kappa$ -carrageenan and 2–4  $\mu\text{m}$  for  $\iota$ -carrageenan) with inclusions containing an increased concentration of carrageenan and protein (Figure 7). The inclusions were up to 40 and 20  $\mu\text{m}$  in diameter for  $\kappa$ - and  $\iota$ -carrageenan,

respectively. We interpret these inclusions as the initiation of bridging flocculation, arrested by gelation.

The microstructure of gels made using a low dosage of hybrid-carrageenan was extensively flocculated with large aggregates (>100  $\mu\text{m}$  in diameter, Figure 5: HM1). The continuous phase exhibited a fine-stranded structure of protein and carrageenan as seen for  $\kappa$ - and  $\iota$ -carrageenan at low dosages. The edges of the aggregates were irregular and composed of smaller subunits.

High dosages of  $\iota$ -,  $\kappa$ -, and hybrid-carrageenan resulted in gels with protein flocculation (Figures 5 and 6: KM2, IM2,

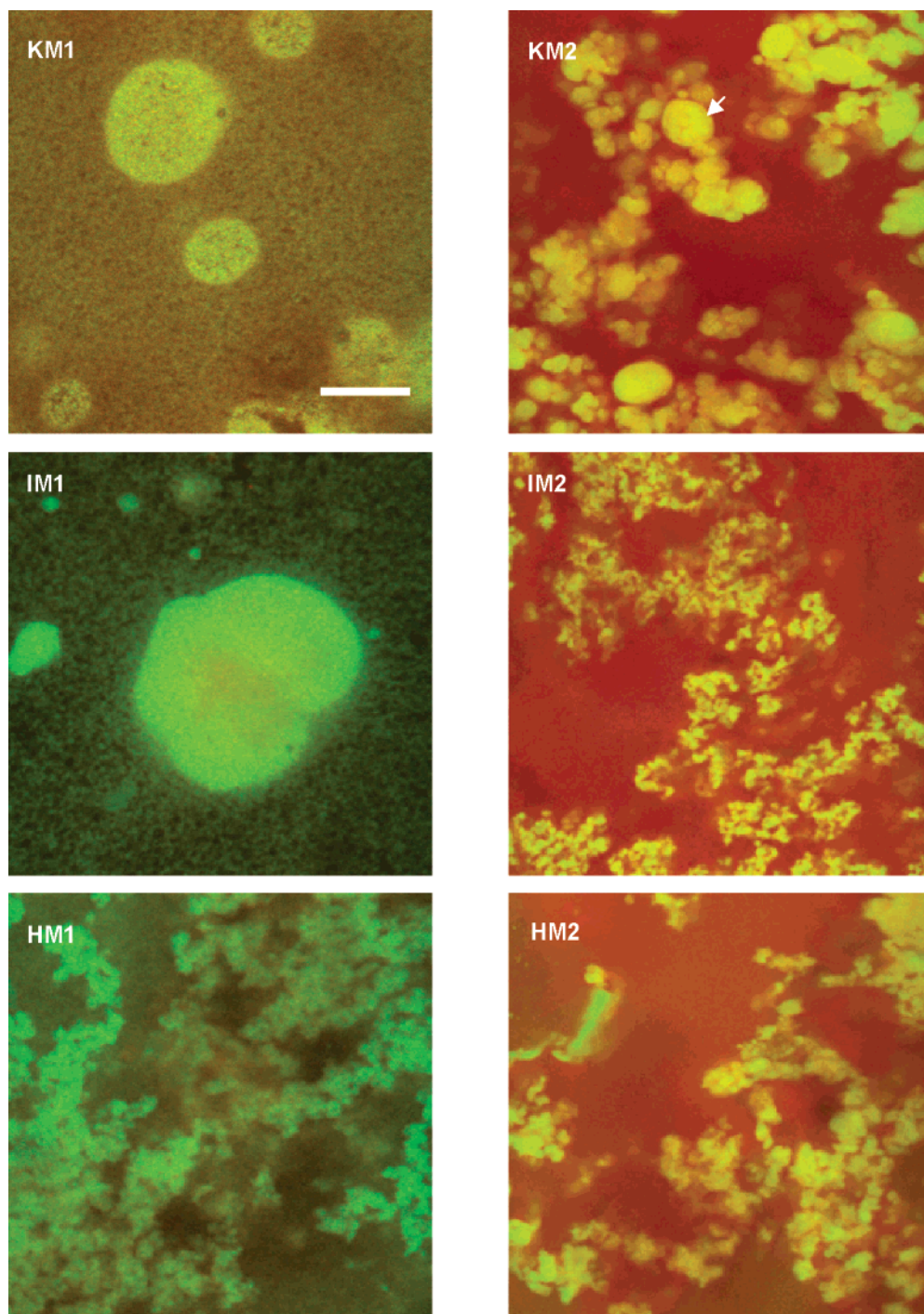


**Figure 6.** Representative high magnification CLSM images of the microstructure of carrageenan-milk gels. Abbreviations as in Table 1. Scale bar represents 20  $\mu\text{m}$ . Green is protein stained with FITC. Red is carrageenan stained with Alexa Fluor 633 conjugated anti-carrageenan antibody. All images have the same magnification as KM1. The arrow in KM2 indicates the subunit with protein concentrated in the center and more carrageenan at the periphery.

and HM2), which was arrested by gelation of the carrageenan phase. However, the carrageenan continuous phase showed a low protein concentration, and carrageenan staining was also present on the aggregates, as illustrated for the low dosage  $\kappa$ -carrageenan gel in Figure 7. The aggregates occupied a major part of the images and were evenly distributed. Differences in the microstructure between the high dosage of  $\iota$ - and  $\kappa$ -carrageenan were observed for the size, shape, and connectivity of the subunits composing the aggregates. When  $\kappa$ -carrageenan was applied in high dosage, each spherical subunit ( $\sim 8 \mu\text{m}$  in diameter) appeared fluffy with a smooth edge and was distinctly separated from the next subunit (Figure 6: KM2). Furthermore,

several of these subunits appeared to have protein concentrated in the center with a higher concentration of carrageenan evident in the periphery. In comparison, the subunits present in the equivalent  $\iota$ -carrageenan gels were smaller ( $\sim 1 \mu\text{m}$ ) and appeared denser, with an irregular edge and were interconnected to a higher degree. The aggregates in the high dosage of hybrid-carrageenan appeared as a mixture of the  $\iota$ - and  $\kappa$ -carrageenan structures (Figure 6: HM2). The continuous phase of  $\kappa$ -,  $\iota$ -, and hybrid-carrageenan high dosage gels was predominantly composed of a pure carrageenan gel.

The negative control antibody was evenly distributed in the samples wherever physically and chemically possible (results



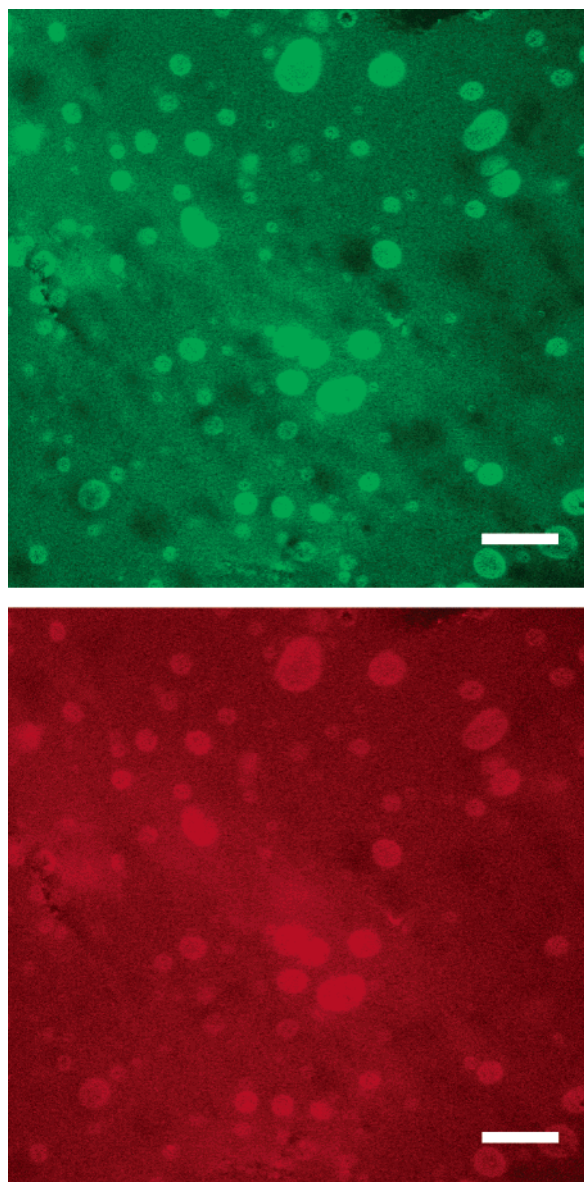


**Figure 7.** Single channel CLSM images of milk based 0.2%  $\kappa$ -carrageenan gel. Scale bar represents 50  $\mu\text{m}$ . Green is the channel showing protein stained with FITC. Red is the channel showing carrageenan stained with Alexa Fluor 633 conjugated anti-carrageenan antibody. The figure illustrates how the staining intensity of both protein and carrageenan increases in the inclusions.

not shown). Thus, the structure imaged by use of the anti-carrageenan antibody-Alexa Fluor 633 conjugate evidently stems from specific binding.

### Discussion

The  $\kappa$ -,  $\iota$ -, and hybrid-carrageenans all responded differently to the dosage increase with respect to changes in firmness, depth at fracture, melting profile, and microstructure, which indicates differences in the mode and impact of the interaction between the casein micelle and the three carrageenan types.

**$\kappa$ -Carrageenan.** The  $\kappa$ -carrageenan gels showed a steeper melting gradient and a higher gel strength as compared to the other gels studied.

Most studies investigating the interaction between casein micelles and  $\kappa$ -carrageenan have been performed at concentrations below 0.03% carrageenan.<sup>5,7,15,16</sup> A majority of studies show interactions between  $\kappa$ -carrageenan and casein only when

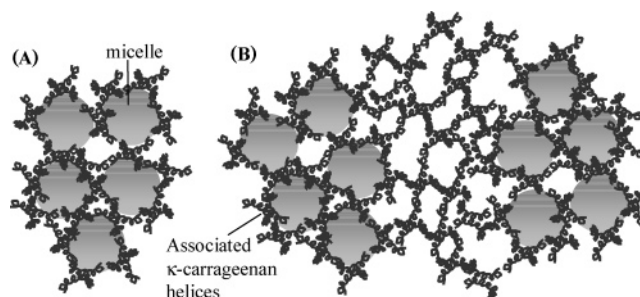


**Figure 8.** Schematic presentation of the  $\kappa$ -carrageenan–milk gel microstructures of (A) 0.2%  $\kappa$ -carrageenan. The associated  $\kappa$ -carrageenan helices interact with the micelles, but the interaction dominating the gel characteristics is the  $\kappa$ -carrageenan– $\kappa$ -carrageenan interaction between the associated helices. Additional gel strength is imposed by the interaction between the associated helices and the micelles (B) 0.7%  $\kappa$ -carrageenan. Flocculated micelles held together by a saturation layer of  $\kappa$ -carrageenan associated helices. The gel characteristics are dominated by  $\kappa$ -carrageenan interactions.

$\kappa$ -carrageenan is in the ordered helix form, indicating that the higher charge density of the helix form is a prerequisite.<sup>5,7,15,16</sup>  $\kappa$ -Carrageenan has a low coil-to-helix transformation temperature ( $\sim 25^\circ\text{C}$  at 0.2% in 0.2 M NaCl), and the gelation point coincides with the coil-to-helix temperature.<sup>2,24</sup> This convergence of the coil-to-helix and gelation temperature leaves little time and mobility for bond formation with  $\kappa$ -casein. In addition, it has also been shown that the interaction of  $\kappa$ -carrageenan with sodium caseinate has little effect on the carrageenan's coil-to-helix transition.<sup>25</sup>

We suggest that in the  $\kappa$ -carrageenan–milk gels, associated  $\kappa$ -carrageenan helices interacted with the micelles. This interaction can be assumed to strengthen the gel network, modify the melting behavior and increase the compatibility between carrageenan and protein. However, when saturation of the micelle surface is reached by bridging flocculation and additional carrageenan is present, flocculation will occur.<sup>5,6,26,27</sup> We thus propose that at the low dosage of  $\kappa$ -carrageenan in milk, the continuous phase was composed of micelle aggregates with associated  $\kappa$ -carrageenan helices at the surface. Even though the carrageenan interacted with the micelle surface, it was carrageenan–carrageenan interactions holding the gel together (Figure 8A). This could explain the fine structure observed in the continuous phase (Figures 5 and 6: KM1) and the only slightly less steep melting profile of the low dosage  $\kappa$ -carrageenan gels as compared to the high dosage  $\kappa$ -carrageenan (Figure 4). The inclusions were of the same composition, only pushed more together due to flocculation. The structure proposed in Figure 8A is supported by several studies.<sup>16,25,28</sup> A slightly less steep melting profile of  $\kappa$ -carrageenan in milk as compared to  $\kappa$ -carrageenan in water was observed by Oakenfull et al.<sup>25</sup> Moreover, a gel composed of more than 0.018%  $\kappa$ -carrageenan in milk exhibits characteristics dominated by carrageenan–carrageenan interactions.<sup>28</sup> Last, in a 0.03–0.1%  $\kappa$ -carrageenan–milk gel, the casein micelles can move over short distances and diffuse at very short time scales,<sup>16</sup> indicating that the micelles are not firmly bound to the  $\kappa$ -carrageenan network.

In the high dosage  $\kappa$ -carrageenan–milk gel, associated  $\kappa$ -carrageenan helices bridged the micelles, and the remaining helices induced flocculation. Thus, a saturation layer of  $\kappa$ -carrageenan can be assumed to be present on the surface of micelles or micellar aggregates,<sup>5,14,26,27</sup> causing formation of a smooth boundary layer toward the continuous  $\kappa$ -carrageenan phase (Figure 6: KM2 and Figure 8B).

The observed difference in microstructure and melting behavior between  $\kappa$ -carrageenan at high and low dosage can

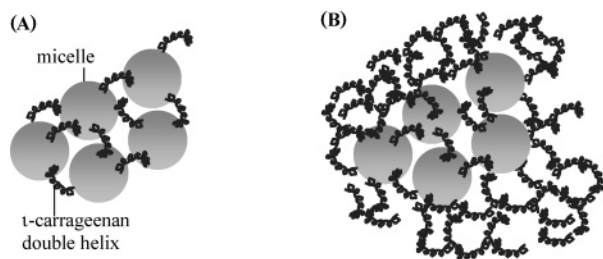


**Figure 9.** Schematic presentation of the  $\iota$ -carrageenan–milk gel microstructure at (A) 0.25%  $\iota$ -carrageenan. The gel is dominated by  $\iota$ -carrageenan–micelle interactions and (B) 1.0%  $\iota$ -carrageenan. Above the saturation layer of  $\iota$ -carrageenan helices, the micelles are flocculated by the remaining  $\iota$ -carrageenan helices. The gel properties are dominated by  $\iota$ -carrageenan– $\iota$ -carrageenan interactions.

be assumed to be the combined result of two factors: the interaction of associated  $\kappa$ -carrageenan helices with the micelles and flocculation of the micelles. At the low dosage of carrageenan where the micelles are least flocculated and the surface area of the micelles is highest, the interaction between associated double helices of  $\kappa$ -carrageenan and micelles dominates the microstructure and decreases the steepness of the melting profile.

**$\iota$ -Carrageenan.** The results indicated that using  $\iota$ -carrageenan in milk at low dosage resulted in a gel with different properties from the other gels studied. The melting profile of low dosage  $\iota$ -carrageenan in milk was different from the other carrageenan gel melting profiles. A much more gradual decrease in  $G^*$  was observed (Figure 4), concurrent with the findings of others.<sup>6,29,30</sup> Furthermore, the gel strength increased less than 2-fold by increasing the  $\iota$ -carrageenan dosage 4-fold, and penetration depth did not significantly differ between the low dosage and the high dosage (Figures 1–3), although the low dosage gel showed decreased critical stress (Figure 3).

The coil-to-helix temperature for 0.5%  $\iota$ -carrageenan in milk permeate is  $\sim 47^\circ\text{C}$ ,<sup>14</sup> which most probably occurs prior to gelation, as the gel setting temperature has been reported to be  $38.5^\circ\text{C}$  for 0.56%  $\iota$ -carrageenan in milk permeate.<sup>6</sup> Additionally,  $\iota$ -carrageenan helices do not aggregate during gelation.<sup>3,4</sup> Hence, before the solution gels, the  $\iota$ -carrageenan helix is rigid enough to possess sufficiently low entropy to approach and interact with the casein micelle. This concurs with the finding that  $\iota$ -carrageenan only interacts with the casein micelle when in the helix form,<sup>6,9</sup> due to its high charge density.<sup>4</sup> The fine-stranded microstructure of the low dosage  $\iota$ -carrageenan–milk gel indicated interaction. We propose that a true coupled network between casein micelles and  $\iota$ -carrageenan was formed as a consequence of  $\iota$ -carrageenan helices interacting with the casein micelles (Figure 9A).

A pure  $\iota$ -carrageenan gel must be weaker than a coupled network of casein and  $\iota$ -carrageenan, as a 4-fold increase in  $\iota$ -carrageenan dosage resulted in a less than 2-fold increase in gel strength (Figures 1 and 3). Indications of different interactions dominating the milk gel properties of  $\kappa$ - and  $\iota$ -carrageenan at low dosage are that the low dosage  $\iota$ -carrageenan–milk gel hardly melted, whereas low dosage  $\kappa$ -carrageenan did melt. These observations have been made previously.<sup>6,25,30</sup> Furthermore, other studies have shown that for  $\iota$ -carrageenan, the gelation temperature is increased in milk as compared to milk permeate, whereas the gelation temperature for  $\kappa$ -carrageenan does not change.<sup>6,14,25</sup> The  $\iota$ -carrageenan helices do not aggregate,<sup>4</sup> which in combination with their higher charge density, may explain why  $\iota$ -carrageenan gels are more prone for formation of a true coupled network with the casein micelles (Figures 1 and 3).<sup>31</sup> Thus, we suggest that at the low dosage of

$\iota$ -carrageenan in milk, the interaction that dominated the gel characteristics was the interaction between the  $\iota$ -carrageenan helix and the micelle, whereas for  $\kappa$ -carrageenan at low and high dosage in milk, the interaction that dominated the gel characteristics was the binding between the associated  $\kappa$ -carrageenan helices and not the interaction between the associated  $\kappa$ -carrageenan helices and the micelle. The interaction between carrageenan and the micelles could be caused by specific electrostatic interactions between carrageenan and the positively charged patch on  $\kappa$ -casein,<sup>9,11,12</sup> or it could be mediated by the calcium present in milk,<sup>32,33</sup> but it could also be mediated by hydrogen bonding or hydrophobic interactions. Whether the interaction of the  $\iota$ - and  $\kappa$ -carrageenan helices to the micelle occurs by the same mechanism seems unlikely but remains to be investigated.

At the high dosage of  $\iota$ -carrageenan flocculation occurred, when a saturation layer of  $\iota$ -carrageenan had formed, and a  $\iota$ -carrageenan– $\iota$ -carrageenan gel constituted the continuous phase (Figures 5 and 6: IM2 and Figure 9B), as when using  $\kappa$ -carrageenan.

**Hybrid-Carrageenan.** Hybrid-carrageenan has a broad coil-to-helix transition temperature,<sup>34</sup> which indicates that the transition is more difficult due to the uneven charge distribution.<sup>1</sup> Since no interaction with the casein micelles occurs with either  $\kappa$ - or  $\iota$ -carrageenan on the coil form,<sup>5,7,15,16</sup> only the limited areas of the hybrid-carrageenan molecules on helix form will interact with the micelles. The melting profiles of the hybrid-carrageenan gels were gradual, in keeping with melting profiles assessed in aqueous solutions where hybrid-carrageenan exhibited a less steep melting gradient than  $\kappa$ -carrageenan.<sup>34</sup>

In contrast to both  $\iota$ - and  $\kappa$ -carrageenan, very large aggregates ( $>100\ \mu\text{m}$ ) were observed in the gels made from the low dosage hybrid-carrageenan. We suggest that for hybrid-carrageenan, initial bridging flocculation occurred, prior to a build-up of sufficient micelle–carrageenan interactions able to arrest further flocculation. On the basis of the microstructure of the continuous phase at low dosage (Figure 5: HM1 arrow) and the melting behavior (Figure 4), we propose that both interaction of the  $\kappa$ - and interaction of the  $\iota$ -carrageenan parts of the hybrid-carrageenan molecules with the casein micelles occurred. But, a limited number of helices was available, and the hybrid-carrageenan on the coil form may have interfered with the gel formation. We further suggest that a gradual melting profile may have two causes: (i) a true coupled network between the  $\iota$ -helices and casein creating a gel that is barely fusible and (ii) the various types of helices in hybrid-carrageenan present involved in a number of different interactions (i.e.,  $\iota$ -carrageenan– $\iota$ -carrageenan,  $\kappa$ -carrageenan– $\kappa$ -carrageenan, or  $\kappa$ -carrageenan–protein) and hence melt at different temperatures. The gradual melting profiles for the hybrid-carrageenan in milk at high and low dosage occurred as a combined result of i and ii. Most likely, i was more important at the low dosage hybrid-carrageenan in milk. A highly schematic presentation of the microstructure of low dosage hybrid-carrageenan in milk is shown in Figure 10. The proposed microstructure is in agreement with the textural profiles of hybrid-carrageenan milk gels showing a strongly decreased gel strength as compared to physical blends of  $\iota$ - and  $\kappa$ -carrageenan of the same composition,<sup>35</sup> probably due to the mixed parts of the hybrid-carrageenan molecules that cannot do the coil-to-helix transformation.

The high dosage of hybrid-carrageenan displayed an abrupt decrease in  $G^*$  between 50 and  $60^\circ\text{C}$  (Figure 4), emulating the melting profile of low dosage  $\kappa$ -carrageenan. This melting behavior was probably due to the 5% contamination of



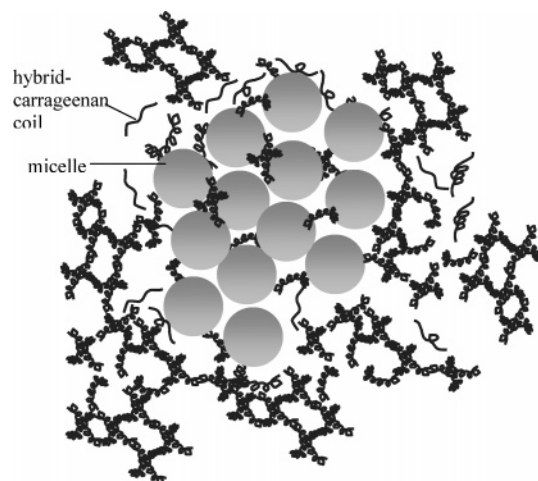


**Figure 10.** Schematic presentation of 0.25% hybrid-carrageenan–milk gel microstructure. Bridging flocculation induced phase separation. The continuous phase is composed of  $\kappa$ -carrageenan areas of the hybrid-carrageenan forming associated helices and  $\iota$ -carrageenan areas of the hybrid-carrageenan forming a gel.

$\kappa$ -carrageenan present in the hybrid-carrageenan. A comparable dominant influence of a small amount of  $\kappa$ -carrageenan contamination has been shown.<sup>35</sup> In addition, at the high dosage of hybrid-carrageenan, proportionally more helices can be assumed to be present, arresting the developing microstructure at a less flocculated stage. The microstructure observed at high dosage of hybrid-carrageenan in milk appeared to be a mixture of characteristics from both the high dosage of  $\iota$ -carrageenan and the high dosage of  $\kappa$ -carrageenan milk gels. Also, at the high dosage of hybrid-carrageenan in milk, bridging flocculation was induced by a number of  $\iota$ -carrageenan helices and associated  $\kappa$ -carrageenan helices bridging the micelles. The continuous phase was thus predominantly a carrageenan gel, and the aggregates were micellar casein aggregates held together by  $\iota$ -carrageenan helices and/or associated  $\kappa$ -carrageenan helices.

Staining of the proteinaceous aggregates with the anti-carrageenan antibody, as seen in Figure 7, indicated that bridging flocculation induced the flocculation, so an initial adsorbed layer of carrageenan can be assumed to be present on the surface of the micelle.<sup>5,14,26,27</sup>

### Conclusion

In conclusion,  $\kappa$ - and  $\iota$ - and hybrid-carrageenan interacted with casein micelles, but they did so with different impacts that determined the resulting microstructures and textures. At low dosages of  $\iota$ -carrageenan, the interaction dominant for the gel characteristics was the interaction between the  $\iota$ -carrageenan helices and the micelles creating a coupled network stronger than a pure  $\iota$ -carrageenan gel. For  $\kappa$ -carrageenan at low dosages, the  $\kappa$ -carrageenan– $\kappa$ -carrageenan interactions dominated the gel characteristics, probably because these interactions melt and break before the  $\kappa$ -carrageenan–micelle interactions. Still, the  $\kappa$ -carrageenan micelle interactions strengthened the gel network. In the case of hybrid-carrageenan, the coil-to-helix transition is difficult due to the mixed molecules. Thus, as only a limited number of helices was present, large aggregates appeared as a consequence of extensive bridging flocculation, occurring before the formation of a continuous network, which arrested the flocculation. These mechanisms can explain the differences found in concentration dependence, thermal behavior, rheology, and microstructure between gels made using the three types of carrageenan in milk. At high dosage  $\iota$ -,  $\kappa$ -, and hybrid-carrageenan, bridging flocculation of the micelles occurred and

induced flocculation of the milk protein, so the gels were dominated by carrageenan–carrageenan interactions.

### References and Notes

- (1) van de Velde, F.; Peppelman, H. A.; Rollema, H. S.; Tromp, R. H. *Carbohydr. Res.* **2001**, *331* (3), 271.
- (2) van de Velde, F.; Antipova, A. S.; Rollema, H. S.; Burova, T. V.; Grinberg, N. V.; Pereira, L.; Gilsenan, P. M.; Tromp, R. H.; Rudolph, B.; Grinberg, V. Y. *Carbohydr. Res.* **2005**, *340* (6), 1113.
- (3) Yuguchi, Y.; Thuy, T. T. T.; Urakawa, H.; Kajiwar, K. *Food Hydrocolloids* **2002**, *16* (6), 515.
- (4) Yuguchi, Y.; Urakawa, H.; Kajiwar, K. *Food Hydrocolloids* **2003**, *17* (4), 481.
- (5) Schorsch, C.; Jones, M. G.; Norton, I. T. *Food Hydrocolloids* **2000**, *14* (4), 347.
- (6) Langendorff, V.; Cuvelier, G.; Launay, B.; Michon, C.; Parker, A.; de Kruif, C. G. *Food Hydrocolloids* **1999**, *13* (3), 211.
- (7) Martin, A. H.; Goff, D. H.; Smith, A.; Dalgleish, D. G. *Food Hydrocolloids* **2006**, *20* (6), 817.
- (8) Snoeren, T. H. M.; Both, P.; Schmidt, D. G. *Neth. Milk Dairy J.* **1976**, *30* (2), 132.
- (9) Dalgleish, D. G.; Morris, E. R. *Food Hydrocolloids* **1988**, *2* (4), 311.
- (10) de Vries, J. Interactions of Carrageenan with Other Ingredients in Dairy Dessert Gels. In *Gums and Stabilizers for the Food Industry, Volume 11*; Williams, P. A., Ed.; Royal society of Chemistry: Cambridge, 2002; pp 201–210.
- (11) Snoeren, T. H. M.; Payens, T. A. J.; Jeunink, J.; Both, P. *Milchwissenschaft* **1975**, *30* (7), 393.
- (12) Payens, T. A. J. *J. Dairy Sci.* **1972**, *55* (2), 141.
- (13) Puvanthiran, A.; Goddard, S. J.; Augustin, M. A. *J. Food Sci.* **2002**, *67* (2), 573.
- (14) Langendorff, V.; Cuvelier, G.; Launay, B.; Parker, A. *Food Hydrocolloids* **1997**, *11* (1), 35.
- (15) Langendorff, V.; Cuvelier, G.; Michon, C.; Launay, B.; Parker, A.; de Kruif, C. G. *Food Hydrocolloids* **2000**, *14* (4), 273.
- (16) Alexander, M.; Dalgleish, D. G. *Food Hydrocolloids* **2006**, *21* (1), 128.
- (17) Spagnuolo, P. A.; Dalgleish, D. G.; Goff, H. D.; Morris, E. R. *Food Hydrocolloids* **2005**, *19* (3), 371.
- (18) Bourriot, S.; Garnier, C.; Doublier, J. L. *Carbohydr. Polym.* **1999**, *40* (2), 145.
- (19) van de Velde, F.; Weinbreck, F.; Edelman, M. W.; van der Linden, E.; Tromp, R. H. *Colloids Surf., B* **2003**, *31* (1–4), 159.
- (20) Arloft, D.; Madsen, F.; Ipsen, R. *Food Hydrocolloids* **2006**, doi: 10.1016/j.foodhyd.2006.07.20.
- (21) Harlow, E.; Lane, D. Staining Tissues. In *Using Antibodies*; Harlow, E., Lane, D., Eds.; Cold Spring Harbor Laboratory Press: New York, 1999; p 151.
- (22) Keller, R.; Winde, G.; Terpe, H. J.; Foerster, E. C.; Domschke, W. *Endoscopy* **2002**, *34* (10), 801.
- (23) Wichmann, J.; Christensen, T. M. I. E.; de Vries, J. Distribution of Kappa and Iota Structures in Hybrid Carrageenans. In *Gums and Stabilizers for the Food Industry, Vol. 13*; Williams, P. A., Ed.; Royal Society of Chemistry: Cambridge, 2006; p 61.
- (24) Piculell, L. Gelling Carrageenans. In *Food Polysaccharides and their Applications*; Stephen, A. M., Ed.; Marcel Dekker: New York, 1995; p 205.
- (25) Oakenfull, D.; Miyoshi, E.; Nishinari, K.; Scott, A. *Food Hydrocolloids* **1999**, *13* (6), 525.
- (26) Hunter, R. J. Effect of Polymers on Colloid Stability. In *Foundations of Colloid Science*; Oxford University Press: Oxford, 2001; p 628.
- (27) Syrbe, A.; Bauer, W. J.; Klostermeyer, N. *Intl. Dairy J.* **1998**, *8* (3), 179.
- (28) Drohan, D. D.; Tziboula, A.; McNulty, D.; Horne, D. S. *Food Hydrocolloids* **1997**, *11* (1), 101.
- (29) Garnier, C.; Michon, C.; Durand, S.; Cuvelier, G.; Doublier, J.-L.; Launay, B. *Colloids Surf., B* **2003**, *31* (1–4), 177.
- (30) Abbasi, S.; Dickinson, E. *J. Agric. Food Chem.* **2004**, *52* (6), 1705.
- (31) Morris, E. R.; Rees, D. A.; Robinson, G. *J. Mol. Biol.* **1980**, *138* (2), 349.
- (32) Skura, B. J.; Nakai, S. *Can. Inst. Food Sci. Technol. J.* **1981**, *14* (1), 59.
- (33) Skura, B. J.; Nakai, S. *J. Food Sci.* **1980**, *45* (3), 582.
- (34) Wang, Q.; Rademacher, B.; Sedlmeyer, F.; Kulozik, U. *Innovative Food Sci. Emerg. Technol.* **2005**, *6* (4), 465.
- (35) Parker, A.; Brigand, G.; Miniou, C.; Trespoey, A.; Vallee, P. *Carbohydr. Polym.* **1993**, *20* (4), 253.